Molecular Therapy
Nucleic Acids
Original Article

miR-25 Promotes Cardiomyocyte Proliferation by Targeting *FBXW7*

Bei Wang,[1,9] Mengting Xu,[2,9] Miaomiao Li,[1] Fujian Wu,[3] Shijun Hu,[4] Xiangbo Chen,[5,6] Liqun Zhao,[7] Zheyong Huang,[8] Feng Lan,[3] Dong Liu,[2] and Yongming Wang[1,2]

[1]State Key Laboratory of Genetic Engineering, School of Life Sciences, Zhongshan Hospital, Fudan University, Shanghai 200438, China; [2]School of Life Sciences, Co-innovation Center of Neuroregeneration, Jiangsu Key Laboratory of Neuroregeneration, Nantong University, Nantong 226001, China; [3]Beijing Anzhen Hospital, Beijing Institute of Heart Lung and Blood Vessel Disease, Capital Medical University, Beijing 100029, China; [4]Institute for Cardiovascular Science & Department of Cardiovascular Surgery of the First Affiliated Hospital, Soochow University, Suzhou 215007, China; [5]Key Laboratory of Molecular Epigenetics of the Ministry of Education (MOE), Northeast Normal University, Changchun 130024, China; [6]Hangzhou Rongze Biotechnology, Hangzhou 310000, Zhejiang, China; [7]Department of Cardiology, Shanghai General Hospital, Shanghai Jiao Tong University School of Medicine, Shanghai 200080, China; [8]Department of Cardiology, Zhongshan Hospital, Fudan University, Shanghai 200032, China

Induction of endogenous cardiomyocyte (CM) proliferation is one of the key strategies for heart regeneration. Increasing evidence points to the potential role of microRNAs (miRNAs) in the regulation of CM proliferation. Here, we used human embryonic stem cell (hESC)-derived CMs (hESC-CMs) as a tool to identify miRNAs that promote CM proliferation. We profiled miRNA expression at an early stage of CM differentiation and identified a list of highly expressed miRNAs. Among these miRNAs, miR-25 was enriched in early-stage hESC-CMs, but its expression decreased over time. Overexpression of miR-25 promoted CM proliferation. RNA sequencing (RNA-seq) analysis revealed that genes related to cell-cycle signal were strongly influenced by miR-25 overexpression. We further showed that miR-25 promoted CM proliferation by targeting *FBXW7*. Finally, the function of miR-25 in the regulation of CM proliferation was demonstrated in zebrafish. Our study suggested that miR-25 is a promising molecule for heart regeneration.

INTRODUCTION

Ischemic cardiomyopathy, one of the most common cardiac myopathies, originates because of inadequate oxygen and nutrient supply, causing myocardial infarction (MI).[1] Adult mammalian cardiomyocytes (CMs) retain only limited endogenous renewal capacity,[2,3] which is insufficient for the replacement of acute or chronic CM loss in ischemic cardiac injury.[3] Several cell-based therapeutic approaches have been developed to treat ischemic heart diseases, including tissue engineering, stem cell transplantation, and mobilization of resident bone marrow cells, but ineffectiveness in clinical applications has fueled disenchantment with these approaches.[4] The ability to use various combinations of cellular reprogramming transcription factors and other agents to directly transdifferentiate fibroblasts into CM-like cells offers a promising approach to treat MI,[5,6] but the resistance of human cells to reprogramming is an important barrier to the clinical application of this strategy.[7]

An alternative, stimulation of endogenous CM proliferation, has emerged as an attractive option for promoting myocardial regeneration. Recent compelling evidence shows that pre-existing CMs in adult mammals have the potential to divide at a very low rate, and myocardial injury can increase the division rate.[8] A more recent study has shown that mature adult CMs can reenter the cell cycle and form new CMs through dedifferentiation, proliferation, and redifferentiation.[9] Increasing evidence points to the potential role of microRNAs (miRNAs) in the regulation of CM proliferation. miRNAs are a class of regulatory RNAs that measure ~22 nt in length and post-transcriptionally regulate the expression of numerous genes via mRNA degradation and translational inhibition.[10,11] Studies in rodents have identified several miRNAs that are involved in CM proliferation.[9,12–16] For example, both miR-590 and miR-199a promote CM proliferation by targeting *Homer1* and *Hopx*,[12] miR-204 promotes CM proliferation by targeting *Jarid2*,[15] and miR-210 promotes CM proliferation by targeting APC.[16] These studies demonstrate that miRNAs play a crucial role in regulating CM proliferation.

Previous studies on CM proliferation have primarily used rodent models. However, the degree to which conclusions can be translated from rodents to human is unknown. Human pluripotent stem cells (hPSCs), including human induced pluripotent stem cells (hiPSCs) and human embryonic stem cells (hESCs),[17,18] can be efficiently differentiated into CMs,[8,19,20] offering a good opportunity to study

Received 29 November 2019; accepted 9 January 2020;
https://doi.org/10.1016/j.omtn.2020.01.013.

[9]These authors contributed equally to this work.

Correspondence: Yongming Wang, State Key Laboratory of Genetic Engineering, School of Life Sciences, Zhongshan Hospital, Fudan University, Shanghai 200438, China.
E-mail: ymw@fudan.edu.cn
Correspondence: Dong Liu, School of Life Sciences, Co-innovation Center of Neuroregeneration, Jiangsu Key Laboratory of Neuroregeneration, Nantong University, Nantong 226001, China.
E-mail: tom@ntu.edu.cn
Correspondence: Feng Lan, Beijing Anzhen Hospital, Beijing Institute of Heart Lung and Blood Vessel Disease, Capital Medical University, Beijing 100029, China.
E-mail: fenglan@ccmu.edu.cn

This is an open access article under the CC BY-NC-ND license (http://creativecommons.org/licenses/by-nc-nd/4.0/).

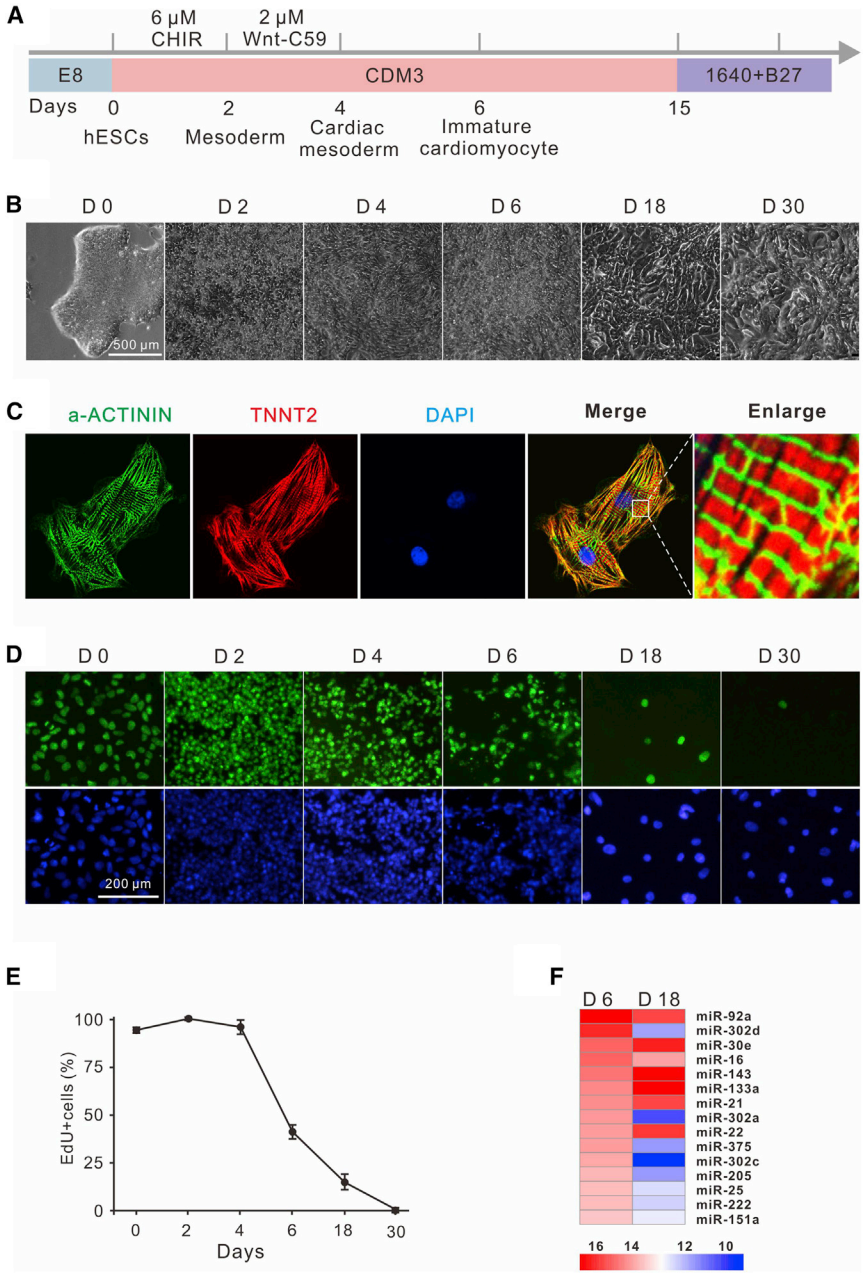

Figure 1. miR-25 Is Enriched in the Early Stage of CM Differentiation

(A) Schematic of chemically defined CM differentiation *in vitro*. (B) The morphology of cells during CM differentiation. (C) Thirty-day-old CMs showed regular sarcomeric structures, as illustrated by immunofluorescent staining of α-ACTININ (green) and TNNT2 (red). (D and E) Cell proliferation decreased from days 4 to 30 as revealed by EdU staining (D). EdU incorporation was quantified using ImageJ software (E). Approximately 2,000 cells were counted in each group. (F) The top 15 most abundant miRNAs at day 6 and their expression levels at day 18 were analyzed by miRNA-seq during hESC differentiation.

RESULTS

Profiling miRNA Expression in the Early Stage of CM Differentiation

Previous studies have shown that early hPSC-CMs proliferate efficiently, similar to embryonic or fetal mammalian CMs, but their capacity for proliferation decreases over time,[22–24] which offers us an opportunity to study which miRNAs regulate CM proliferation during this process. We used a monolayer-differentiation method to generate hPSC-CMs by temporally manipulating the canonical Wnt signaling pathway (Figure 1A). The CM transition requires several intermediate stages including mesoderm (day 2), cardiac mesoderm (day 4), and CM progenitor cells (day 6).[19,25] The marker gene expression of each stage was confirmed by quantitative reverse transcription polymerase chain reaction (qRT-PCR) (Figure S1). The morphology of cells changed over time during differentiation (Figure 1B). Eight days after differentiation, the cells started contracting rhythmically (Video S1). Thirty days after differentiation, CMs showed regular sarcomeric structures, as illustrated by immunofluorescent (IF) α-actinin (α-ACTININ), cardiac troponin T (TNNT2), and 4′,6′-diamidino-phenylindole (DAPI) staining (Figure 1C). A 5-ethynyl-2′-deoxyuridine (EdU) cell proliferation assay revealed that cell proliferation decreased from 95.7% at day 4 to 1.9% at day 30 (Figures 1D and 1E).

CM proliferation in human cells. A recent large-scale screening using hPSC-derived CMs revealed that proliferative miRNAs in humans overlapped only minimally with those previously shown to stimulate rodent CM proliferation.[21] In this study, we profiled miRNA expression at an early stage of CM differentiation and identified a list of highly expressed miRNAs. Further screening showed that *miR-25* overexpression promotes CM proliferation. Importantly, we identified *FBXW7* as a target of miR-25 for the promotion of CM proliferation. Our study suggests that miR-25 could be a potential molecule for cardiac regeneration.

We hypothesized that miRNAs with high expression levels played a key role in regulating CM proliferation during CM differentiation. We profiled miRNA expression at the genome-wide level at two time points: days 6 and 18. We focused on miRNAs that highly expressed on day 6 but dramatically changed at day 18 (fold change >2 for upregulation, fold change <0.5 for downregulation) and identified 15 miRNAs. Among these miRNAs, expression of miR-30e,

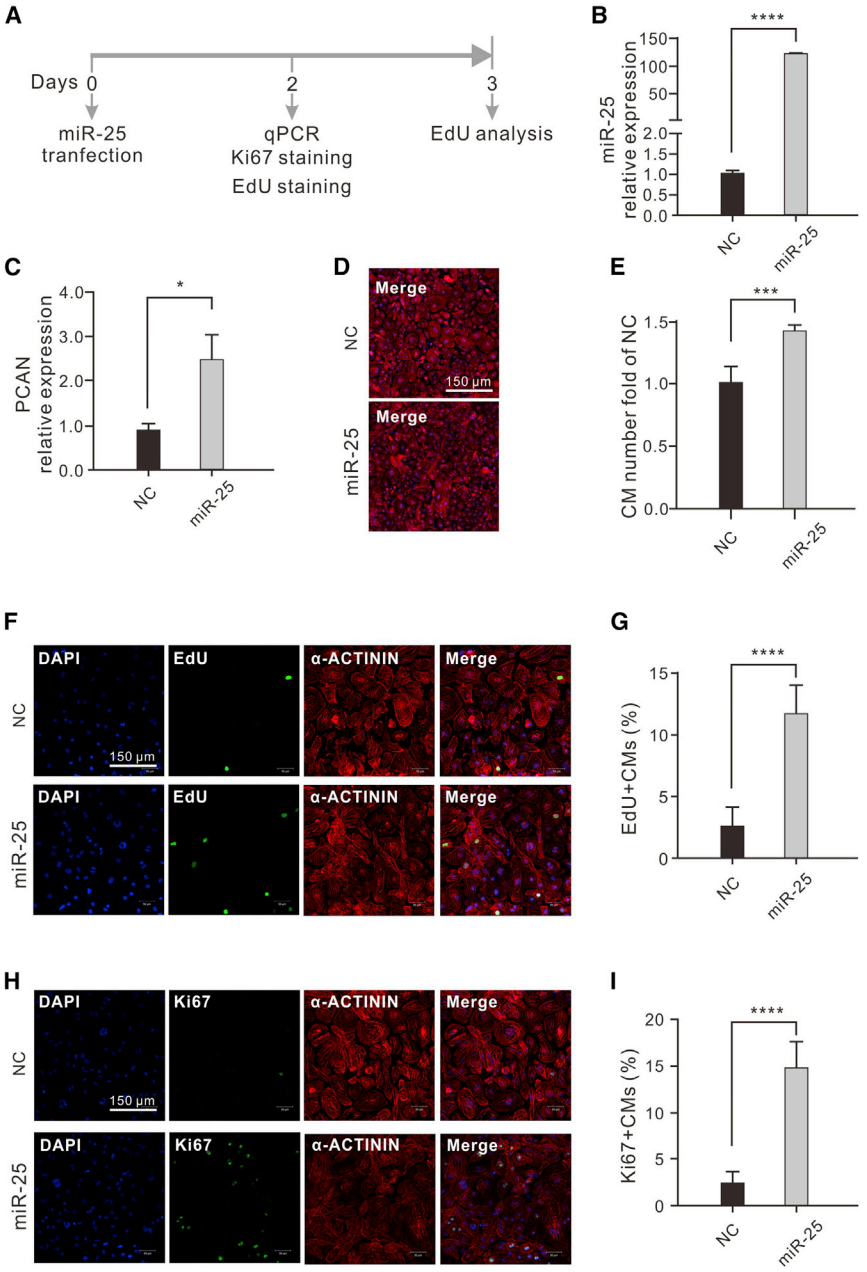

Figure 2. miR-25 Promotes hESC-CM Proliferation

(A) Schematic of the experimental design. (B) qRT-PCR analysis showed that miR-25 expression was significantly increased in hESC-CMs transfected with miR-25 mimics (n = 3) NC = cells transfected with normal control mimics. (C) qRT-PCR analysis showed that the expression of proliferating cell nuclear antigen (PCNA) increased in hESC-CMs transfected with miR-25 mimics (n = 3). NC = cells transfected with normal control mimics. (D) hESC-CMs transfected with miR-25 mimics or NC were stained for sarcomeric α-ACTININ (red) and DAPI (blue). (E) Relative numbers of hESC-CMs treated with miRNA-25 or NC. (n = 3) (F) hESC-CMs transfected with miR-25 mimics or NC were stained with EdU (green), an antibody against α-ACTININ (red) and DAPI (blue). (F) Percentage of Edu^+ hESC-CMs treated with miR-25 mimics or NC. Approximately 2,000 cells were counted in each group. (H) hESC-CMs transfected with miR-25 mimics or NC were stained with an antibody against Ki-67 (green), α-ACTININ (red) and DAPI (blue). (I) Percentage of $Ki\text{-}67^+$ hESC-CMs treated with miR-25 mimics or NC. Approximately 2,000 cells were counted in each group. Statistical significance was calculated using Student's t test for paired samples. Data are shown as the mean ± SEM. *$p < 0.05$, ***$p < 0.001$, ****$p < 0.0001$.

miR-143, miR-133a, miR-21, and miR-22 increased, whereas expression of miR-92a, miR-302/367 cluster, miR-16, miR-375, miR-205, miR-25, miR-222, and miR-151a decreased (Figure 1F). We hypothesized that the change of these miRNA expressions was associated with CM proliferation. Interestingly, miR-92a, miR-302/367 cluster, miR-16, miR-133, and miR-222 have been shown to regulate CM proliferation.[13,26–29]

Overexpression of miR-25 Promotes hESC-CM Proliferation

To identify additional miRNAs that promote CM proliferation, we knocked down miR-30e, miR-143, miR-21, and miR-22 in the 30-day-old hESC-CMs, but none of these miRNAs could promote CM proliferation. We overexpressed miR-375, miR-25, miR-205, and miR-151a in the 30-day-old hESC-CMs, and EdU cell proliferation assay revealed that miR-25 significantly promoted CM proliferation (Figure 2A; Figure S2). qRT-PCR showed that transfection of miR-25 mimics led to overexpression of miR-25 (Figure 2B) and proliferating cell nuclear antigen (PCNA) (Figure 2C). Transfection of miR-25 mimics led to CM proliferation as indicated by cell counts (Figures 2D and 2E). The proliferation of CMs was confirmed by an EdU cell proliferation assay. miR-25 transfection led to an increase in EdU-positive hESC-CMs from 2.5% to 11.6% (Figures 2F and 2G). We also used Ki-67 immunostaining to investigate the proliferation of CMs. The proportion of Ki-67-positive cells increased from 2.3% to 14.6% after miR-25 transfection (Figures 2H and 2I). In addition to its effect on hESC-CMs, miR-25 also promoted the proliferation of hiPSC-derived CMs (hiPSC-CMs) (Figures S3A–S3D). In summary, overexpression of miR-25 could promote proliferation of both hESC-CMs and hiPSC-CMs.

We further examined whether overexpression of miR-25 influenced other properties of CMs. Overexpression of miR-25 did not influence sarcomeric structure (Figure S4A), cell size (Figures S4A and S4B), field potential duration (FPD; Fridericia corrected) (Figures S4C and S4D), or beat period (Figure S4E).

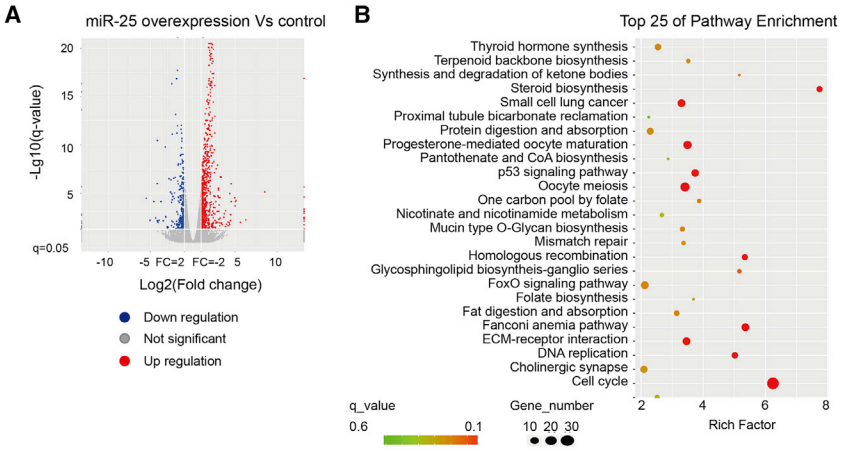

Figure 3. miR-25 Overexpression Drives Cell-Cycle Progression in hESC-CMs

(A) Volcano map for the 967 differentially expressed genes in hESC-CMs overexpressing miR-25 compared with the normal control. (B) Scatterplots of the top 25 differentially regulated pathways identified in KEGG analyses. The vertical axis is the pathway term; the horizontal axis shows the rich factor for KEGG pathway enrichment. The q value denotes the significance of the pathway item. (C) qRT-PCR analysis revealed that miR-25 overexpression increased the expression of cell proliferation-associated genes and cell-cycle-related genes (n = 3). Statistical significance was calculated using Student's t test for paired samples. Data are shown as the mean ± SEM. *p < 0.05, **p < 0.01, ***p < 0.001, ****p < 0.0001.

To better understand the molecular and cellular effects of miR-25 overexpression, we performed RNA sequencing (RNA-seq) analysis. A total of 967 differentially expressed genes (DEGs; q value < 0.05) were identified, including 696 upregulated genes and 271 downregulated genes (Figure 3A). Kyoto Encyclopedia of Genes and Genomes (KEGG) enrichment analysis showed that 30 upregulated genes belonged to pathways related to the cell cycle, 16 genes were related to oocyte meiosis, and 10 genes were related to the p53 signaling pathway (Figure 3B). KEGG classification analysis showed that the most affected classes of genes were related to signal transduction, cancers, and cell growth and death (Figure S5A). Gene Ontology (GO) analysis revealed that the DEGs enriched in cellular components were related to proliferation, including condensed chromosome kinetochores and biological processes such as DNA replication (Figure S5B). qRT-PCR revealed that the expression of cell proliferation-associated genes (*BRCA2*, *NUSAP1*, *RACGAP1*, and *CKS2*) and cell-cycle-related genes (*CCNA2*, *CCNB*, *CCND*, *CDK2*, and *E2F2*) was increased (Figure 3C). These results indicated that miR-25 overexpression partly activated some cell-cycle-related genes that promote CM proliferation.

miR-25 Regulates hESC-CM Proliferation by Targeting *FBXW7*

To elucidate the mechanism of miR-25 in the regulation of CM proliferation, we used TargetScan and miRTarBase to predict miR-25 target genes. We focused on candidate targets that were predicted by both tools and obtained a list of 165 genes. Among these genes, *BTG2*, *RECK*, *LATS2*, *CDKN1C*, and *FBXW7* have been reported to promote cancer cell proliferation.[15,30–33] A dual-luciferase reporter assay was performed to test whether these genes were direct targets of miR-25 in HEK293T cells. We constructed reporter constructs containing luciferase fused with the wild-type (WT) 3′ UTR of each gene. An initial screen revealed that fusion with the 3′ UTR of *RECK*, *LATS2*, and *CDKN1C* did not influence luciferase activity, whereas fusion with the 3′ UTR of *BTG2* and *FBXW7* decreased luciferase activity (Figures 4A and 4B; Figures S6A–S6H), suggesting that *BTG2* and *FBXW7* could be direct targets of miR-25. However, knockdown of *BTG2* by small interfering RNA (siRNA) did not promote CM proliferation (Figure S7).

One miR-25 binding site was predicted on the *FBXW7* 3′ UTR (Figure 4A). The luciferase reporter assay revealed that miR-25 abolished the inhibitory effect when this site was mutated, indicating that it was an miR-25 binding site (Figure 4B). To investigate whether miR-25 inhibits *FBXW7* in CMs, we transfected miR-25 mimics into CMs, which resulted in downregulation of *FBXW7* expression as revealed by qRT-PCR (Figure 4C) and western blotting (Figures 4D and 4E). To test whether downregulation of *FBXW7* expression led to CM proliferation, we transfected an siRNA against *FBXW7* (siFBXW7) into hESC-CMs. Downregulation of *FBXW7* expression was confirmed by qRT-PCR (Figure 4F). *FBXW7* knockdown led to an increase in *PCNA* expression (Figure 4G), a marker gene of cell proliferation. Moreover, transfection of siFBXW7 led to hESC-CM proliferation as indicated by EdU and Ki-67 staining (Figures 4H and 4I). Taken together, these results demonstrated that miR-25 promoted hESC-CM proliferation at least partially via inhibition of *FBXW7*.

miR-25 Promotes CM Proliferation in Zebrafish

To investigate the regenerative potential of miR-25 at the organ level, we employed transgenic zebrafish with myocardium-specific GFP

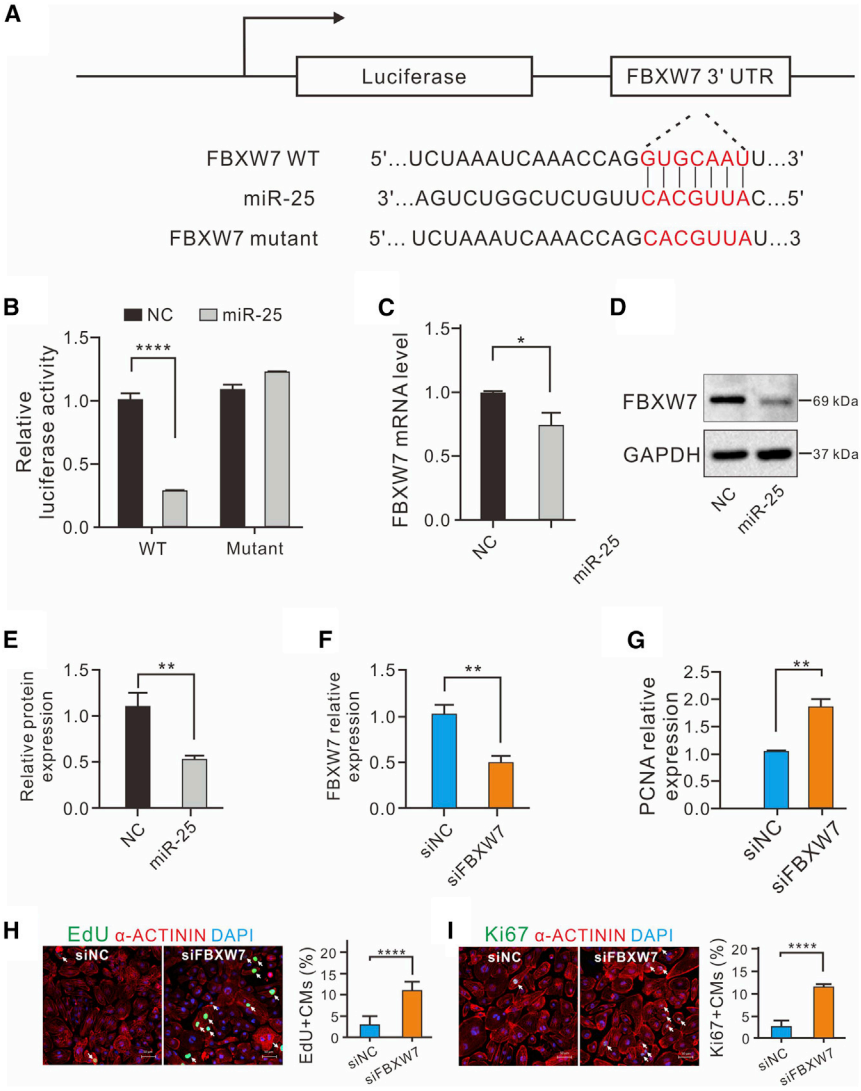

Figure 4. *FBXW7* Is a Direct Target Gene of miR-25

(A) A potential target site (highlighted in red) of miR-25 on the *FRXW7* 3′ UTR was predicted by TargetScan. The mutated target sequence is shown below. (B) A luciferase reporter assay showed that the predicted binding sequence was required for miR-25 inhibition (n = 3). (C) qRT-PCR showed that miR-25 overexpression decreased *FBXW7* expression in hESC-CMs (n = 3). (D) Western blot analysis showed that miR-25 overexpression decreased FBXW7 expression in hESC-CMs. (E) Fold change expression of FBXW7 normalized by GAPDH as a internal control in hESC-CMs treated with miR-25 mimics or NC. (n = 3). (F) *FBXW7* expression was knocked down by siFBXW7 in hESC-CMs (n = 3). (G) qRT-PCR showed that PCNA expression was significantly increased in hESC-CMs treated with siFBXW7 (n = 3). (H) EdU staining (green) revealed that *FBXW7* knockdown increased CM proliferation. The number of EdU-positive cells is shown on the right. Nuclei were stained with DAPI (blue); CMs were stained with an antibody against α-ACTININ (red). Approximately 2,000 cells were quantified in each group. Scale bars, 150 μm. (I) Ki-67 staining (green) revealed that *FBXW7* knockdown increased CM proliferation. The number of Ki-67-positive cells is shown on the right. Nuclei were stained with DAPI (blue); CMs were stained with an antibody against α-ACTININ (red). Approximately 2,000 cells were quantified in each group. Scale bars, 150 μm. Mut, mutant; siNC, siRNA negative control; WT, wild-type. Statistical significance was calculated using student's t test for paired samples. Data are shown as the mean ± SEM. *$p < 0.05$, **$p < 0.01$, ***$p < 0.001$, ****$p < 0.0001$.

expression. miR-25 or normal control (NC) mimics were injected into the single-cell stage of zebrafish embryos. Heart morphology, size, and CM number were examined 72 h postfertilization (hpf). Confocal imaging revealed that miR-25 injection resulted in enlargement of the heart compared with the NC group (Figure 5A). Consistent with confocal imaging analysis, histological section analysis revealed that miR-25 injection significantly increased the cross-sectional area (Figures 5B and 5C). Furthermore, we analyzed the CM size by miR-25 injection, and the results revealed that miR-25 injection increased CM size (Figures 5D and 5E). To investigate whether CM number contributed to heart enlargement, we employed another transgenic zebrafish line with myocardium-specific RFP expression in the nuclei. Interestingly, miR-25 injection increased the number of CMs (Figures 5F and 5G), and it displayed a more significant effect on the proliferation of atrium CMs (Figure S8). Neither miR-25 nor NC injection had any influence on heart rate (Figure 5H). Collectively, these data demonstrated that miR-25 injection could increase both the size and the number of CMs in zebrafish.

miR-25 Targets *fbxw7* in Zebrafish

To test whether miR-25 targeted *fbxw7* in zebrafish as well, we carried out a series of experiments. First, the sequence alignment analysis demonstrated that the zebrafish miR-25 (dre-miR-25) mature sequence was identical to the human miR-25 (hsa-miR-25) (Figure 6A). Moreover, we found that dre-miR-25 potentially targeted *fbxw7* in zebrafish through TargetScanFish prediction (Figure 6B). *In vitro* luciferase assays revealed that miR-25 duplex significantly inhibited the expression of luciferase-*fbxw7*-3′ UTR compared with that of the control (Figure 6C). To test the functional interaction of miR-25 and *fbxw7*-3′ UTR *in vivo*, we performed the fluorescence sensor assay in zebrafish embryos. It was confirmed that miR-25 mimics repressed the expression of the mCherry-*fbxw7*-3′ UTR, but not mCherry-*fbxw7*-3′ UTR-mutant (mut), in which the miR-25 potential targeting site was mutated (Figure 6D). In summary, these results demonstrated that miR-25 also targeted *fbxw7* in zebrafish.

DISCUSSION

Direct activation of endogenous CM proliferation to regenerate and repair the heart, both after injury and in chronic disease states, is

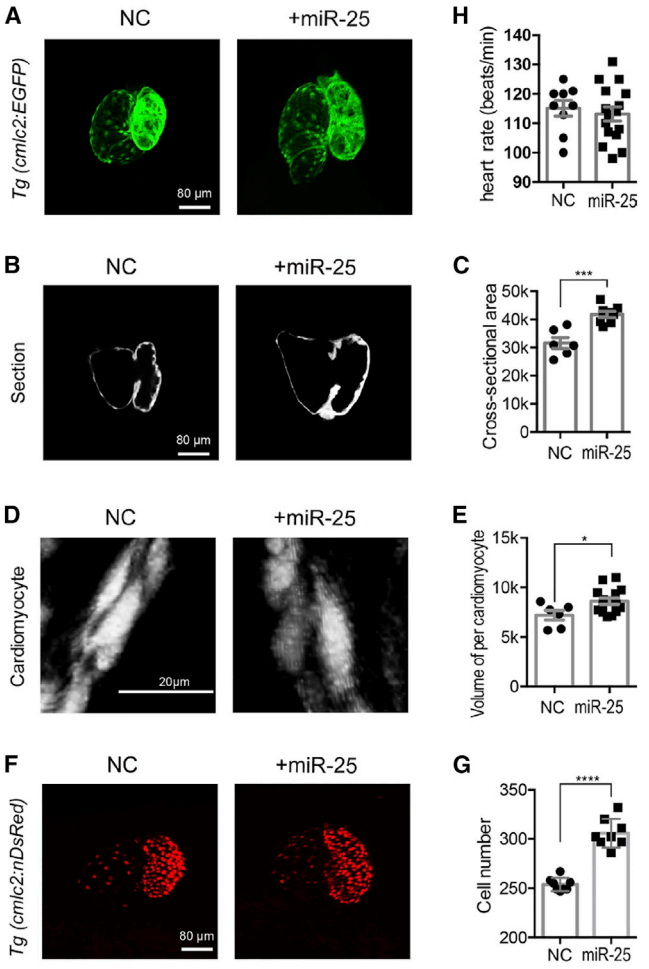

Figure 5. miR-25 Promotes CM Proliferation in Zebrafish

(A) Morphology of zebrafish hearts injected with miR-25 mimics or NC. Transgenic zebrafish with myocardium-specific GFP expression were used. (B) Histological section of the cross-sectional areas of miR-25 or NC injection. (C) The cross-sectional areas of miR-25 or NC injection. (n > 6) (D) The confocal picture of single CM injected with miR-25 or NC. (E) The volume of single CM treated with miR-25 or NC. (F) CM of zebrafish hearts injected with miR-25 or NC. (G) The number of CMs after miR-25 or NC injections. A transgenic zebrafish line with myocardium-specific RFP expression in the nuclei was employed. (H) miR-25 injection did not influence heart rate. Statistical significance was calculated using Student's t test for paired samples. Data are shown as the mean ± SEM. *p < 0.05, **p < 0.01, ***p < 0.001, ****p < 0.0001.

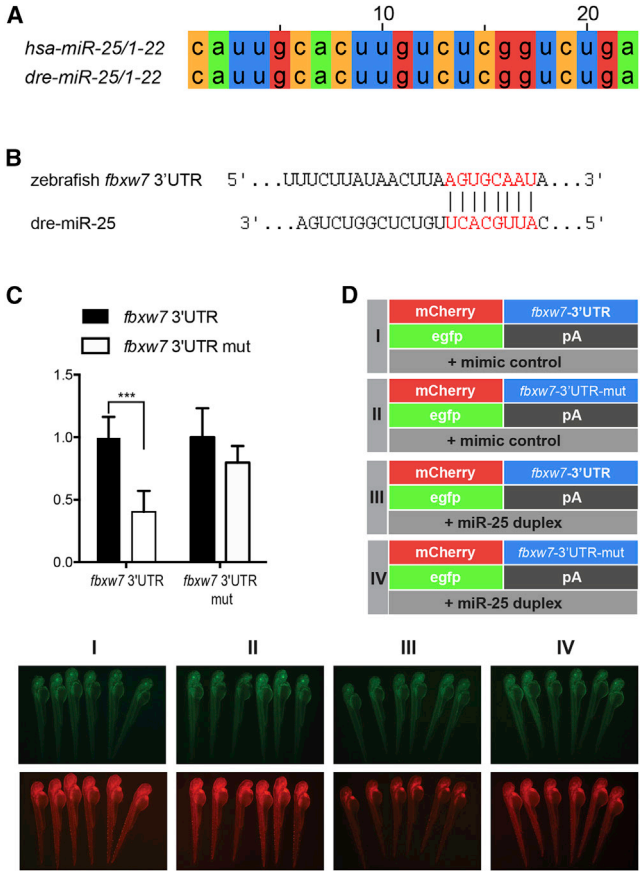

Figure 6. FBXW7 Is a Direct Target Gene of miR-25 in Zebrafish

(A) The sequence of miR-25 sequences is conserved in human and zebrafish. (B) A potential target site (highlighted in red) of miR-25 on the zebrafish *fbxw7* 3′ UTR was predicted by TargetScan. (C) Luciferase reporter assay showed that the predicted binding sequence was required for miR-25 inhibition. (D) mCherry sensors were co-injected with EGFP control as indicated. miR-25-duplex injection reduced the mCherry levels in mCherry-*fbxw7*-3′ UTR, whereas EGFP levels were unchanged. In the mutated sensor, no reduction in mCherry was noted. Experiments were repeated three times; for each group, six embryos were analyzed. Mut, mutant. Statistical significance was calculated using Student's t test for paired samples. Data are shown as the mean ± SEM. *p < 0.05, **p < 0.01, ***p < 0.001, ****p < 0.0001.

emerging as one of the most promising strategies in cardiac regenerative medicine.[34] Identification of genes that can be harnessed to promote CM proliferation would be helpful for cardiac regeneration. Previous studies in rodents revealed that forced overexpression of certain synthetic miRNAs can promote CM proliferation.[12,34] In this study, we harnessed hESC-CMs to decipher miRNA functions in CM proliferation and demonstrated that miR-25 promoted CM proliferation. Importantly, we identified *FBXW7* as a target of miR-25 to regulate human CM proliferation. *FBXW7* is a cell-cycle regulatory factor that mediates the ubiquitin-dependent proteolysis of many positive cell-cycle regulators, including cyclin E1, c-Myc, c-Jun, and Notch.[35,36] Low expression of *FBXW7* has been observed in colorectal cancer.[37] Inactivation of *Fbxw7* in the T cell lineage of mice impairs cell-cycle exit during T cell differentiation.[38] Therefore, *FBXW7* plays an important role in the regulation of cell proliferation by modulating cell-cycle activities. In this study, we demonstrate that *FBXW7* is a target of miR-25, and overexpression of miR-25 promotes CM proliferation by downregulating *FBXW7*. These results were confirmed in the zebrafish model. Therefore, miR-25 could serve as a novel molecule for cardiac regeneration.

miR-25 has multiple effects on heart failure. miR-25 expression in humans is initially decreased in the early stage of heart failure but is later increased in end-stage heart failure.[39] Decreased miR-25 expression in diseased myocardium leads to re-expression of its target gene

Hand2, a transcription factor that can cause cardiac dilation and dysfunction in the postnatal myocardium.[40] Interestingly, another group has demonstrated that inhibition of miR-25 expression in diseased myocardium leads to overexpression of its target gene *SERCA2a* and improves cardiac function.[20] Other effects of miR-25 include protection of CMs against oxidative damage[41] and against apoptosis induced by sepsis.[42] We first demonstrated that miR-25 promoted CM proliferation, extending the list of miR-25 functions.

Notably, multiple effects of miR-25 in the rodent heart have also been documented, some of which seem to contradict each other. Overexpression of miR-25 protects CMs against oxidative damage and sepsis-induced apoptosis.[41,42] On the other hand, overexpression of miR-25 in the normal heart causes a significant loss of contractile function, CM fibrosis, and apoptosis.[20,39] However, this study revealed that overexpression of miR-25 in zebrafish did not significantly alter the heart function. Inhibition of miR-25 improves cardiac contractility in the failing heart[20] but can also induce atrial fibrillation,[43] high blood pressure,[39] mild heart dilation,[39] and spontaneous cardiac dysfunction.[40] Therefore, additional studies are required to investigate the therapeutic effects of the miR-25 expression during different stages of heart disease.

MATERIALS AND METHODS

Cell Culture

The HEK293T (ATCC) cell line was grown in DMEM supplemented with 10% FBS, 1× penicillin-streptomycin. hESCs (Wicell) and hiPSCs (Kindly provided by Cellapy) were maintained in human PSCeasy Medium (Cellapy) on Matrigel-coated (Corning) plates and passaged using 0.5 mM EDTA every ~3–4 days. All cells were incubated at 37°C with 95% air and 5% CO_2.

In Vitro Differentiation

hESCs and hiPSCs were directly differentiated using small molecules following a previously described method.[44] In brief, before differentiation, cells were dissociated using 0.5 mM EDTA at a ratio of approximately 1:10 and cultured in human PSCeasy Medium for ~3–4 days. When the cell density reached ~60%–70% confluence on day 0, the medium was changed to CDM3 basal medium containing 6 μM CHIR99021 (Selleck), an inhibitor of GSK3β that activates the Wnt signaling pathway. On day 2, the medium was changed to CDM3 containing 2 μM Wnt-C59 (Sigma), a Wnt inhibitor. From day 4 onward, the medium was replaced with fresh CDM3 every other day, and spontaneously contracting CMs were observed on day 8. From days 9 to 12, CMs were purified with Cardioeasy purification medium (Cellapy). CMs were maintained with medium composed of RPMI 1640 with 2% B27 serum-free supplement (Gibco) from day 15 onward, with the medium exchanged every 2 or 3 days.

Luciferase Reporter Assay

The 3′ UTR of the target gene containing putative binding sites for miR-25-3p was amplified by PCR from human genomic DNA and inserted into a psiCHECK-2 vector within XhoI and NotI restriction sites. Mutations were introduced in the seed region of the miR-25-3p binding site for comparison. The synthesized pre-miR-25 sequence was cloned into plko.1 to construct the miR-25 expression plasmid. For the luciferase reporter assay, HEK293T cells were preplated in 12-well plates. On the next day, the cells were cotransfected with 500 ng plko-miR-25 or control plasmid and 500 ng WT or mutated 3′ UTR of *FBXW7* using Lipofectamine 2000 reagent (Invitrogen) according to the manufacturer's instructions. After transfection for 48 h, the cell lysates were harvested, and luciferase activity was measured using the Dual-Luciferase Reporter System (Promega). The activity of *Renilla* luciferase was normalized to that of firefly luciferase. The experiment was repeated three times independently.

Immunofluorescence

After 48 h of transfection, CMs were washed with PBS three times for 5 min each and fixed with 4% Paraformaldehyde Fix Solution (Sangon Biotech) for 15 min at room temperature and permeabilized with 0.3% Triton X-100 in PBS for 15 min, then blocked with 3% BSA for 1 h. Next, the cells were incubated with primary antibody in blocking solution overnight at 4°C. The following primary antibodies were used: mouse anti-α-ACTININ (1:500; Sigma) and rabbit anti-TNNT2 (1:500; Proteintech) were used for labeling the CMs. Rabbit anti-Ki-67 (1:300; Cell Signaling) was used to detect mitosis. After being washed with PBS three times, cells were incubated with secondary antibodies conjugated with Alexa Fluor 488 and 584 (Sigma) for 1 h at room temperature in the dark. For EdU staining, CMs were labeled with EdU for 24 h before immunofluorescence, and the Click-iT EdU Alexa Fluor 488 Imaging kit (Invitrogen) was used according to the manufacturer's protocol. DAPI (1:1,000; Sigma) was used to stain nuclei. CM proliferation was calculated by counting Ki-67 $(EdU)^+$, α-$ACTININ^+$, and $DAPT^+$ cells in every image. More than 2000 cells were counted. CM size was quantified using ImageJ.

Oligo Transfection

The synthetic miR-25 mimics, *FBXW7* siRNA, and their NC were purchased from GenePharma (Shanghai). Differentiated CMs were isolated and replated at 80% confluency; after 3 days, when they resumed beating, they were transfected with 40 nM miRNA mimics or siRNA using Lipofectamine 3000 transfection reagent (Invitrogen). After 48 h of treatment, they were used for immunofluorescence, western blot, or qRT-PCR analysis.

RNA Isolation and qRT-PCR

Total RNA (including mRNA and miRNA) was extracted from treated CMs using TRIzol reagent (Ambion) following the manufacturer's manual. For mRNA expression analysis, first-strand cDNA was synthesized using a 5× All-In-One RT MasterMix kit (abm), and mRNA expression was quantified with 2× SYBR Green qPCR Master Mix (bimake) according to the manufacturer's protocol. GAPDH was used as an internal control. For miRNA, the cDNA was reverse transcribed using the miScript II RT kit (QIAGEN). The relative expression level of miR-25-3p was evaluated with the miScript SYBR Green PCR kit (QIAGEN) and normalized to hU6. qPCR was performed using the Bio-Rad Real-Time PCR Detection System, and the relative expression level was calculated using the $2^{-\Delta\Delta Ct}$ method. The primer sequences used can be seen in Table S1.

Western Blot Analysis

Treated cells were harvested and lysed with Nonidet P-40 (NP-40) buffer (Beyotime) in the presence of 1 mM phenylmethanesulfonyl fluoride (Beyotime). After the cells were spun at 12,000 rpm for 10 min in a 4°C precooled centrifuge, the supernatant was collected for western blot analysis. Proteins were separated on an 8% SDS-PAGE gel and then transferred to a polyvinylidene fluoride (PVDF) membrane (Thermo). After being locked with 5% (w/v) BSA (Sigma) in TBS-T (0.1% Tween 20 in 1× TBS) buffer for 1 h at room temperature, the membrane was incubated with primary antibodies at 4°C overnight. The following antibodies were used: anti-FBXW7 (1:1,000; Abcam) and anti-GAPDH (1:2,000; Cell Signaling). After three washes in TBS-T for 5 min each, the membranes were incubated with secondary antibody at room temperature for 1 h, then washed three times and stained following the kit manufacturer's recommendation. ImageJ was used to quantify the band intensities.

RNA-Seq and Bioinformatics Analysis

RNA-seq was performed by Shanghai Biotechnology Corporation (SBC). In brief, CMs transfected with miR-25-3p mimics or its NC were collected, and total RNA was extracted using an RNeasy Micro Kit (QIAGEN) following the manufacturer's instructions. Total RNA integrity was checked with an Agilent Bioanalyzer 2100 (Agilent). The cDNA library was constructed using a TruSeq RNA Sample Prep Kit and sequenced on an Illumina HiSeq 2000 system (Illumina). Sequenced reads were mapped onto the human hg38 reference genome. The reads were converted into FPKM (fragments per kilobase of exon model per million mapped reads) for standardization of gene expression using StringTie (version 1.3.0). EdgeR was applied to identify DEGs between samples. KEGG and GO enrichment were analyzed for differentially expressed genes. The RNA-seq data has been deposited to SRA Database (accession number: PRJNA531900).

Electrical Activity Analysis

A multi-electrode array (MEA; Multi Channel Systems) was utilized to record the electrophysiological features of CMs, including beat period, field potential duration (FPD), and conduction velocity. FPD was subsequently corrected (FPDc) using Fridericia's formula (FDP/3 $\sqrt{RR}$, where RR is the interspike interval). All experiments were performed in DMEM without FBS or antibiotics.

Ethics Statement

All zebrafish experimentation was carried out in accordance with the NIH *Guidelines for the Care and Use of Laboratory Animals* (https://oacu.od.nih.gov/regs/index.htm) and ethically approved by the Administration Committee of Experimental Animals, Jiangsu Province, China (approval ID: SYXK (SU) 2007-0021).

Zebrafish Strains and Breeding

Zebrafish were provided by the Zebrafish Center at Nantong University Jiangsu Key Laboratory of Neuroregeneration. Zebrafish embryos and adults were raised and maintained under the conditions described previously.[45] Two transgenic zebrafish lines, *Tg(cmlc2:nDsRed)* and *Tg(cmlc2:GFP)*, were used as described in a previous work.[45]

Injection of miRNA-25 Mimic and NC

miRNA-25 mimic 20 pmol and NC were injected into embryos in the one- to two-cell stages.

Target Prediction

Target prediction of miR-25 in zebrafish was carried out with TargetScanFish 6.2 (http://www.targetscan.org/fish_62/).

Whole-Embryo miRNA Sensor Assay

A whole-embryo miRNA sensor assay in zebrafish was carried out as described previously.[45] *egfp* and *mCherry* coding sequences were cloned into the pCS2$^+$ vector. The pCS2$^+$-*mCherry-fbxw7*-3′ UTR control and the pCS2$^+$-*mCherry-fbxw7*-3′ UTR-mut construct were generated. The pCS2$^+$-*EGFP* vector was used as an injection control. The plasmids were linearized with NotI/KpnI and used as templates to synthesize the capped mRNAs using a mMESSAGE mMACHINE kit (Ambion). The RNAs were injected into the cytoplasm of one- to two-cell embryos (35 pg/embryo).

Microscopic Imaging

For microscopic imaging of zebrafish, embryos were embedded in 0.6% low-melting point agarose. Confocal imaging was performed with a Leica TCS-SP5 LSM. The anesthetic MS-222 (100% strength) was used to stop the heartbeat before confocal imaging. Analysis was performed using Imaris software.

Statistical Analysis

Statistical analysis was performed using GraphPad Prism 5. All data are presented as the mean ± SEM. An unpaired t test and one-way ANOVA were used to determine statistical significance between two and more than two groups, respectively. Significance levels are indicated as follows: $^*p < 0.05$, $^{**}p < 0.01$, $^{***}p < 0.001$, $^{****}p < 0.0001$.

SUPPLEMENTAL INFORMATION

Supplemental Information can be found online at https://doi.org/10.1016/j.omtn.2020.01.013.

AUTHOR CONTRIBUTIONS

B.W., M.X., M.L., and F.W. designed and performed the experiments; S.H. and X.C. analyzed the miRNA-seq data; F.L., L.Z., and Z.H. revised the manuscript; D.L. and Y.W. supervised the project. All authors read and approved the final manuscript.

CONFLICTS OF INTEREST

X.C. works for Hangzhou Rongze Biotechnology Co., Ltd. The other authors declare no competing interests.

ACKNOWLEDGMENTS

This work was supported by grants from the National Natural Science Foundation of China (grant 81870199); National Basic Research Program of China (grant 2015CB943300); Foundation for Innovative

Research Group of the National Natural Science Foundation of China (grant 31521003); and Opening Program 2018 of the State Key Laboratory of Genetic Engineering (grant SKLGE1809).

REFERENCES

1. Anderson, J.L., and Morrow, D.A. (2017). Acute Myocardial Infarction. N. Engl. J. Med. *376*, 2053–2064.
2. Senyo, S.E., Lee, R.T., and Kühn, B. (2014). Cardiac regeneration based on mechanisms of cardiomyocyte proliferation and differentiation. Stem Cell Res. (Amst.) *13* (3 Pt B), 532–541.
3. Bergmann, O., Bhardwaj, R.D., Bernard, S., Zdunek, S., Barnabé-Heider, F., Walsh, S., Zupicich, J., Alkass, K., Buchholz, B.A., Druid, H., et al. (2009). Evidence for cardiomyocyte renewal in humans. Science *324*, 98–102.
4. Eschenhagen, T., Bolli, R., Braun, T., Field, L.J., Fleischmann, B.K., Frisén, J., Giacca, M., Hare, J.M., Houser, S., Lee, R.T., et al. (2017). Cardiomyocyte Regeneration: A Consensus Statement. Circulation *136*, 680–686.
5. Ieda, M., Fu, J.D., Delgado-Olguin, P., Vedantham, V., Hayashi, Y., Bruneau, B.G., and Srivastava, D. (2010). Direct reprogramming of fibroblasts into functional cardiomyocytes by defined factors. Cell *142*, 375–386.
6. Qian, L., Huang, Y., Spencer, C.I., Foley, A., Vedantham, V., Liu, L., Conway, S.J., Fu, J.D., and Srivastava, D. (2012). In vivo reprogramming of murine cardiac fibroblasts into induced cardiomyocytes. Nature *485*, 593–598.
7. Muraoka, N., Yamakawa, H., Miyamoto, K., Sadahiro, T., Umei, T., Isomi, M., Nakashima, H., Akiyama, M., Wada, R., Inagawa, K., et al. (2014). MiR-133 promotes cardiac reprogramming by directly repressing Snai1 and silencing fibroblast signatures. EMBO J. *33*, 1565–1581.
8. Senyo, S.E., Steinhauser, M.L., Pizzimenti, C.L., Yang, V.K., Cai, L., Wang, M., Wu, T.D., Guerquin-Kern, J.L., Lechene, C.P., and Lee, R.T. (2013). Mammalian heart renewal by pre-existing cardiomyocytes. Nature *493*, 433–436.
9. Deng, S., Zhao, Q., Zhen, L., Zhang, C., Liu, C., Wang, G., Zhang, L., Bao, L., Lu, Y., Meng, L., et al. (2017). Neonatal Heart-Enriched miR-708 Promotes Proliferation and Stress Resistance of Cardiomyocytes in Rodents. Theranostics *7*, 1953–1965.
10. Nair, N., and Gongora, E. (2014). MicroRNAs as therapeutic targets in cardiomyopathies: myth or reality? Biomol. Concepts *5*, 439–448.
11. Palacín, M., Reguero, J.R., Martín, M., Díaz Molina, B., Morís, C., Alvarez, V., and Coto, E. (2011). Profile of microRNAs differentially produced in hearts from patients with hypertrophic cardiomyopathy and sarcomeric mutations. Clin. Chem. *57*, 1614–1616.
12. Eulalio, A., Mano, M., Dal Ferro, M., Zentilin, L., Sinagra, G., Zacchigna, S., and Giacca, M. (2012). Functional screening identifies miRNAs inducing cardiac regeneration. Nature *492*, 376–381.
13. Tian, Y., Liu, Y., Wang, T., Zhou, N., Kong, J., Chen, L., Snitow, M., Morley, M., Li, D., Petrenko, N., et al. (2015). A microRNA-Hippo pathway that promotes cardiomyocyte proliferation and cardiac regeneration in mice. Sci. Transl. Med. *7*, 279ra38.
14. Pandey, R., and Ahmed, R.P. (2015). MicroRNAs Inducing Proliferation of Quiescent Adult Cardiomyocytes. Cardiovasc. Regen. Med. *2*, e519.
15. Liang, D., Li, J., Wu, Y., Zhen, L., Li, C., Qi, M., Wang, L., Deng, F., Huang, J., Lv, F., et al. (2015). miRNA-204 drives cardiomyocyte proliferation via targeting Jarid2. Int. J. Cardiol. *201*, 38–48.
16. Arif, M., Pandey, R., Alam, P., Jiang, S., Sadayappan, S., Paul, A., and Ahmed, R.P.H. (2017). MicroRNA-210-mediated proliferation, survival, and angiogenesis promote cardiac repair post myocardial infarction in rodents. J. Mol. Med. (Berl.) *95*, 1369–1385.
17. Thomson, J.A., Itskovitz-Eldor, J., Shapiro, S.S., Waknitz, M.A., Swiergiel, J.J., Marshall, V.S., and Jones, J.M. (1998). Embryonic stem cell lines derived from human blastocysts. Science *282*, 1145–1147.
18. Takahashi, K., Tanabe, K., Ohnuki, M., Narita, M., Ichisaka, T., Tomoda, K., and Yamanaka, S. (2007). Induction of pluripotent stem cells from adult human fibroblasts by defined factors. Cell *131*, 861–872.
19. Burridge, P.W., Keller, G., Gold, J.D., and Wu, J.C. (2012). Production of de novo cardiomyocytes: human pluripotent stem cell differentiation and direct reprogramming. Cell Stem Cell *10*, 16–28.
20. Wahlquist, C., Jeong, D., Rojas-Muñoz, A., Kho, C., Lee, A., Mitsuyama, S., van Mil, A., Park, W.J., Sluijter, J.P., Doevendans, P.A., et al. (2014). Inhibition of miR-25 improves cardiac contractility in the failing heart. Nature *508*, 531–535.
21. Diez-Cuñado, M., Wei, K., Bushway, P.J., Maurya, M.R., Perera, R., Subramaniam, S., Ruiz-Lozano, P., and Mercola, M. (2018). miRNAs that induce human cardiomyocyte proliferation converge on the hippo pathway. Cell Rep. *23*, 2168–2174.
22. Snir, M., Kehat, I., Gepstein, A., Coleman, R., Itskovitz-Eldor, J., Livne, E., and Gepstein, L. (2003). Assessment of the ultrastructural and proliferative properties of human embryonic stem cell-derived cardiomyocytes. Am. J. Physiol. Heart Circ. Physiol. *285*, H2355–H2363.
23. McDevitt, T.C., Laflamme, M.A., and Murry, C.E. (2005). Proliferation of cardiomyocytes derived from human embryonic stem cells is mediated via the IGF/PI 3-kinase/Akt signaling pathway. J. Mol. Cell. Cardiol. *39*, 865–873.
24. Cui, L., Johkura, K., Takei, S., Ogiwara, N., and Sasaki, K. (2007). Structural differentiation, proliferation, and association of human embryonic stem cell-derived cardiomyocytes in vitro and in their extracardiac tissues. J. Struct. Biol. *158*, 307–317.
25. Liu, Q., Jiang, C., Xu, J., Zhao, M.T., Van Bortle, K., Cheng, X., Wang, G., Chang, H.Y., Wu, J.C., and Snyder, M.P. (2017). Genome-Wide Temporal Profiling of Transcriptome and Open Chromatin of Early Cardiomyocyte Differentiation Derived From hiPSCs and hESCs. Circ. Res. *121*, 376–391.
26. Chen, J., Huang, Z.P., Seok, H.Y., Ding, J., Kataoka, M., Zhang, Z., Hu, X., Wang, G., Lin, Z., Wang, S., et al. (2013). mir-17-92 cluster is required for and sufficient to induce cardiomyocyte proliferation in postnatal and adult hearts. Circ. Res. *112*, 1557–1566.
27. Porrello, E.R., Johnson, B.A., Aurora, A.B., Simpson, E., Nam, Y.J., Matkovich, S.J., Dorn, G.W., 2nd, van Rooij, E., and Olson, E.N. (2011). MiR-15 family regulates postnatal mitotic arrest of cardiomyocytes. Circ. Res. *109*, 670–679.
28. Liu, N., Bezprozvannaya, S., Williams, A.H., Qi, X., Richardson, J.A., Bassel-Duby, R., and Olson, E.N. (2008). microRNA-133a regulates cardiomyocyte proliferation and suppresses smooth muscle gene expression in the heart. Genes Dev. *22*, 3242–3254.
29. Liu, X., Xiao, J., Zhu, H., Wei, X., Platt, C., Damilano, F., Xiao, C., Bezzerides, V., Boström, P., Che, L., et al. (2015). miR-222 is necessary for exercise-induced cardiac growth and protects against pathological cardiac remodeling. Cell Metab. *21*, 584–595.
30. D'Uva, G., Aharonov, A., Lauriola, M., Kain, D., Yahalom-Ronen, Y., Carvalho, S., Weisinger, K., Bassat, E., Rajchman, D., Yifa, O., et al. (2015). ERBB2 triggers mammalian heart regeneration by promoting cardiomyocyte dedifferentiation and proliferation. Nat. Cell Biol. *17*, 627–638.
31. Chen, H., Pan, H., Qian, Y., Zhou, W., and Liu, X. (2018). MiR-25-3p promotes the proliferation of triple negative breast cancer by targeting BTG2. Mol. Cancer *17*, 4.
32. Zhao, H., Wang, Y., Yang, L., Jiang, R., and Li, W. (2014). MiR-25 promotes gastric cancer cells growth and motility by targeting RECK. Mol. Cell. Biochem. *385*, 207–213.
33. Xiang, J., Hang, J.B., Che, J.M., and Li, H.C. (2015). MiR-25 is up-regulated in non-small cell lung cancer and promotes cell proliferation and motility by targeting FBXW7. Int. J. Clin. Exp. Pathol. *8*, 9147–9153.
34. Chen, J., Huang, Z.-P., Seok, H.Y., Ding, J., Kataoka, M., Zhang, Z., Hu, X., Wang, G., Lin, Z., Wang, S., et al. (2013). mir-17–92 cluster is required for and sufficient to induce cardiomyocyte proliferation in postnatal and adult hearts. Circ. Res. *112*, 1557–1566.
35. Minella, A.C., and Clurman, B.E. (2005). Mechanisms of tumor suppression by the SCF(Fbw7). Cell Cycle *4*, 1356–1359.
36. Welcker, M., and Clurman, B.E. (2008). FBW7 ubiquitin ligase: a tumour suppressor at the crossroads of cell division, growth and differentiation. Nat. Rev. Cancer *8*, 83–93.
37. Iwatsuki, M., Mimori, K., Ishii, H., Yokobori, T., Takatsuno, Y., Sato, T., Toh, H., Onoyama, I., Nakayama, K.I., Baba, H., and Mori, M. (2010). Loss of FBXW7, a cell cycle regulating gene, in colorectal cancer: clinical significance. Int. J. Cancer *126*, 1828–1837.

38. Onoyama, I., Tsunematsu, R., Matsumoto, A., Kimura, T., de Alborán, I.M., Nakayama, K., and Nakayama, K.I. (2007). Conditional inactivation of Fbxw7 impairs cell-cycle exit during T cell differentiation and results in lymphomatogenesis. J. Exp. Med. *204*, 2875–2888.

39. Li, H., Xie, Y., Liu, Y., Qi, Y., Tang, C., Li, X., Zuo, K., Sun, D., Shen, Y., Pang, D., et al. (2018). Alteration in microRNA-25 expression regulate cardiac function via renin secretion. Exp. Cell Res. *365*, 119–128.

40. Dirkx, E., Gladka, M.M., Philippen, L.E., Armand, A.S., Kinet, V., Leptidis, S., El Azzouzi, H., Salic, K., Bourajjaj, M., da Silva, G.J., et al. (2013). Nfat and miR-25 cooperate to reactivate the transcription factor Hand2 in heart failure. Nat. Cell Biol. *15*, 1282–1293.

41. Pan, L., Huang, B.J., Ma, X.E., Wang, S.Y., Feng, J., Lv, F., Liu, Y., Liu, Y., Li, C.M., Liang, D.D., et al. (2015). MiR-25 protects cardiomyocytes against oxidative damage by targeting the mitochondrial calcium uniporter. Int. J. Mol. Sci. *16*, 5420–5433.

42. Yao, Y., Sun, F., and Lei, M. (2018). miR-25 inhibits sepsis-induced cardiomyocyte apoptosis by targetting PTEN. Biosci. Rep. *38*, BSR20171511.

43. Chiang, D.Y., Kongchan, N., Beavers, D.L., Alsina, K.M., Voigt, N., Neilson, J.R., Jakob, H., Martin, J.F., Dobrev, D., Wehrens, X.H., and Li, N. (2014). Loss of microRNA-106b-25 cluster promotes atrial fibrillation by enhancing ryanodine receptor type-2 expression and calcium release. Circ. Arrhythm. Electrophysiol. *7*, 1214–1222.

44. Burridge, P.W., Holmström, A., and Wu, J.C. (2015). Chemically defined culture and cardiomyocyte differentiation of human pluripotent stem cells. Curr. Protoc. Hum. Genet. *87*, 21.3.1–21.3.15.

45. Wang, X., Ling, C.C., Li, L., Qin, Y., Qi, J., Liu, X., You, B., Shi, Y., Zhang, J., Jiang, Q., et al. (2016). MicroRNA-10a/10b represses a novel target gene mib1 to regulate angiogenesis. Cardiovasc. Res. *110*, 140–150.

OMTN, Volume *19*

Supplemental Information

miR-25 Promotes Cardiomyocyte Proliferation by Targeting *FBXW7*

Bei Wang, Mengting Xu, Miaomiao Li, Fujian Wu, Shijun Hu, Xiangbo Chen, Liqun Zhao, Zheyong Huang, Feng Lan, Dong Liu, and Yongming Wang

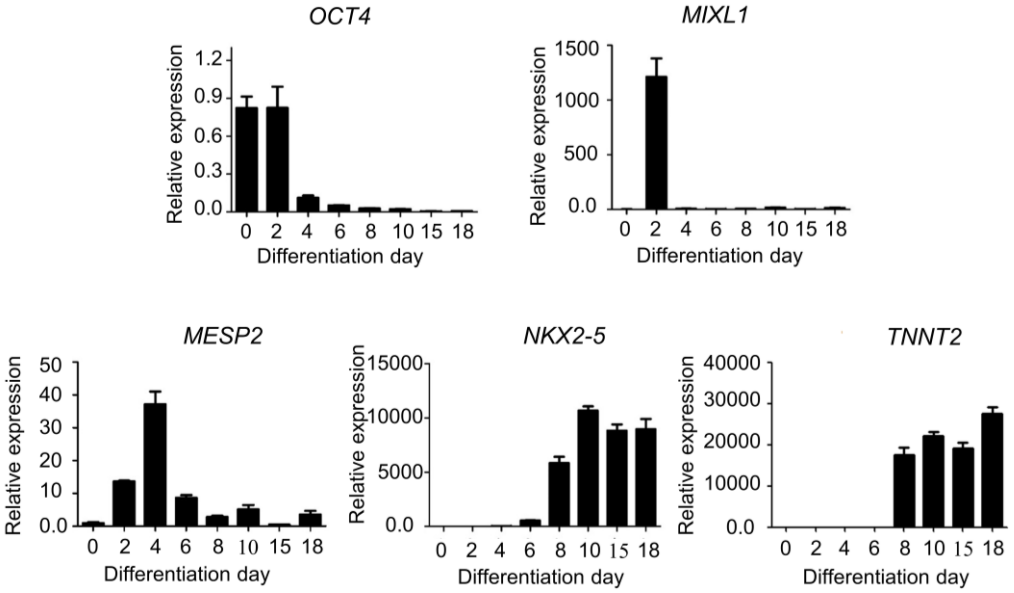

Supplemental Figure 1. Relative mRNA expression levels of marker genes for pluripotent stem cells (*OCT4*), mesendoderm (*MIXL1*), cardiac mesoderm (*MESP1*), cardiac progenitors (*NKX2-5*) and cardiomyocytes (*TNNT2*) were analyzed by qRT-PCR during CM differentiation (n=3, error bars show the mean ± SEM).

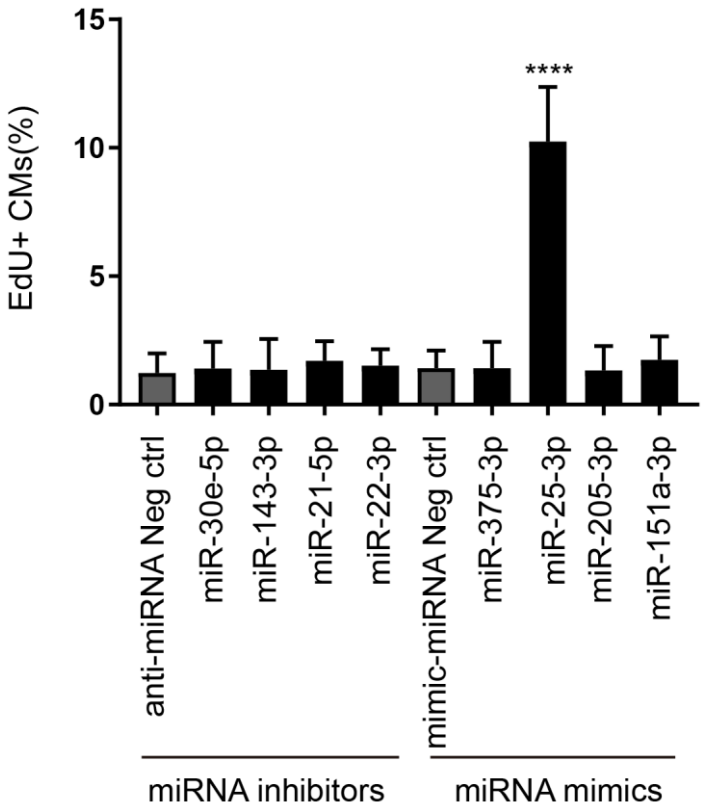

Supplemental Figure 2. Anti-miRNA and mimic-miRNA screen for hESC-CMs proliferation. The percentage of EdU+ and α-ACTININ+ cells were quantificated using ImageJ. (n=3 per group, error bars showed mean± SD).

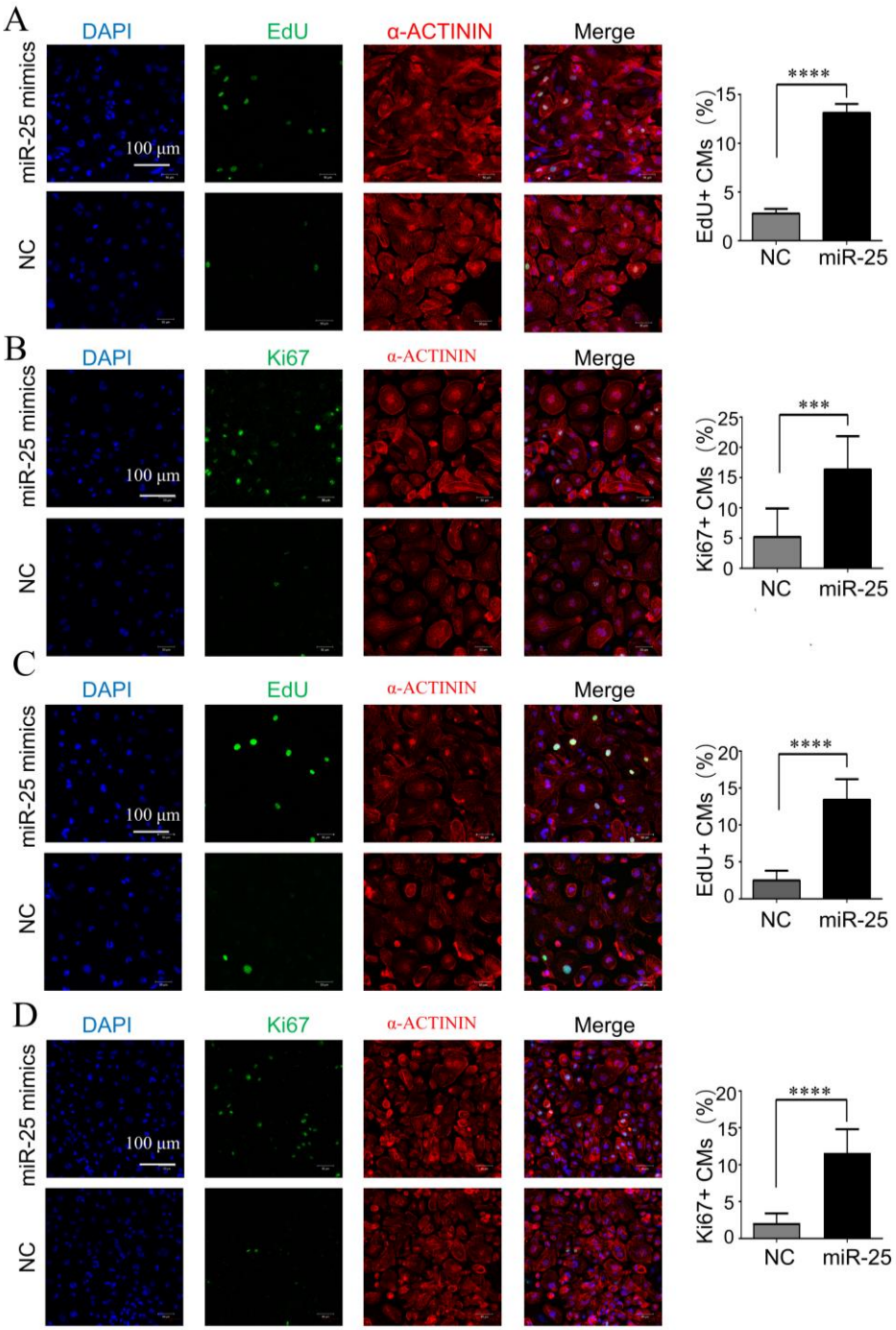

Supplemental Figure 3. miR-25 overexpression promotes the proliferation of CMs derived from two hiPSC lines. (A) EdU staining (green) revealed that miR-25 transfection increased the proliferation of CMs derived from hiPSC line 1. (B) Immunostaining of Ki-67 revealed that miR-25 transfection increased the proliferation of CMs derived from hiPSC line 1. (C) EdU staining (green) revealed that miR-25 transfection increased the proliferation of CMs derived from hiPSC line 2. (D) Immunostaining of Ki-67 revealed that miR-25 transfection increased the proliferation of CMs derived from hiPSC line 2. Nuclei were stained with DAPI (blue); CMs were stained with an antibody against α-ACTININ (red). At least 2000 cells were quantified in each group.

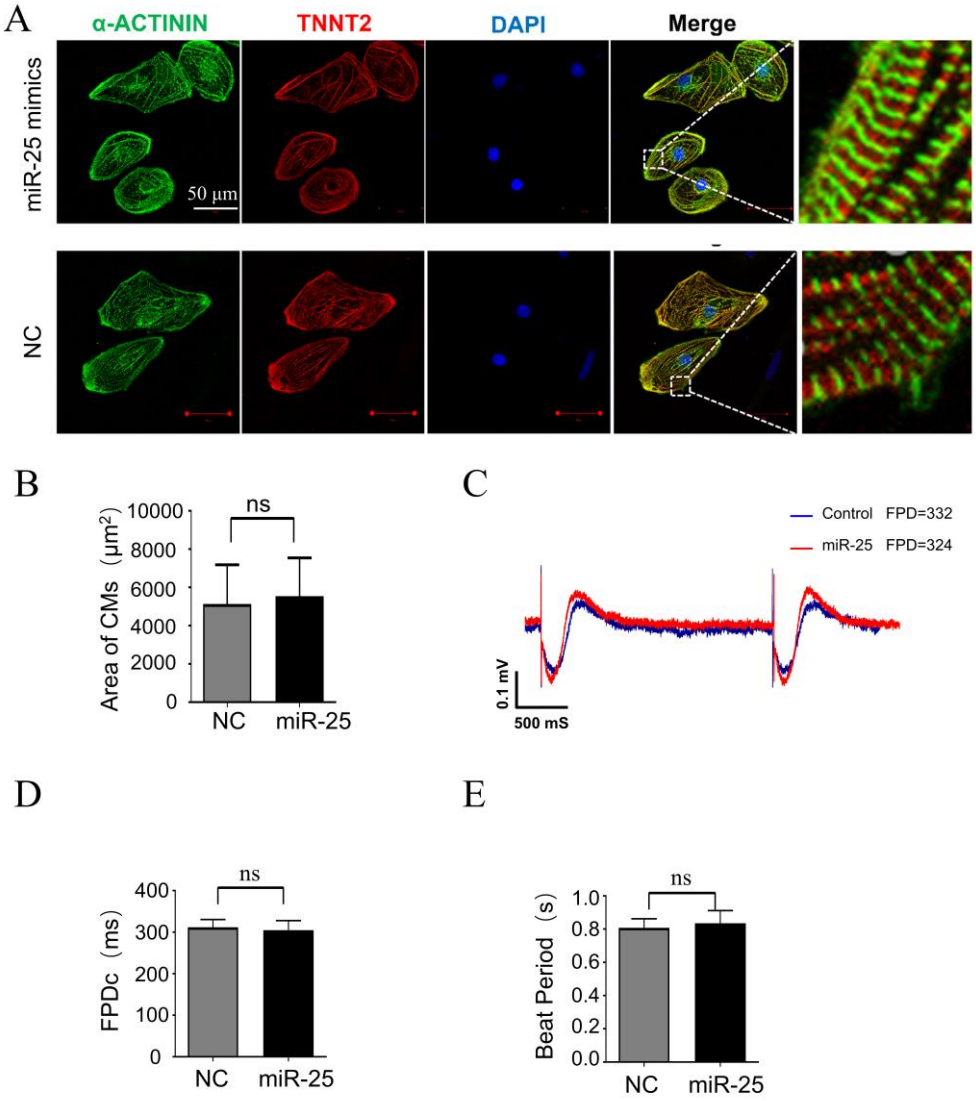

Supplemental Figure 4. Overexpression of miR-25 did not influence CM morphology or electrical activity. (A) Representative images of hESC-CMs transfected with miR-25 mimics or NC stained for α-ACTININ (green), TNNT2 (red) and DAPI (blue). (B) Quantification of cell size. Approximately 60 cells for each group were analyzed. (C) Representative traces of average FPD recordings using the MEA system. (D, E) The results of field potential duration (FPD, Fridericia corrected) and beat period analysis (n=3, error bars show the mean ± SEM).

Supplemental Figure 5. RNA-seq analysis revealed that miR-25 overexpression influenced the expression of multiple genes in hESC-CMs. (A) KEGG classification enrichment analysis of the differentially expressed genes in CMs transfected with miR-25. (B) GO enrichment analysis of the differentially expressed genes in CMs transfected with miR-25.

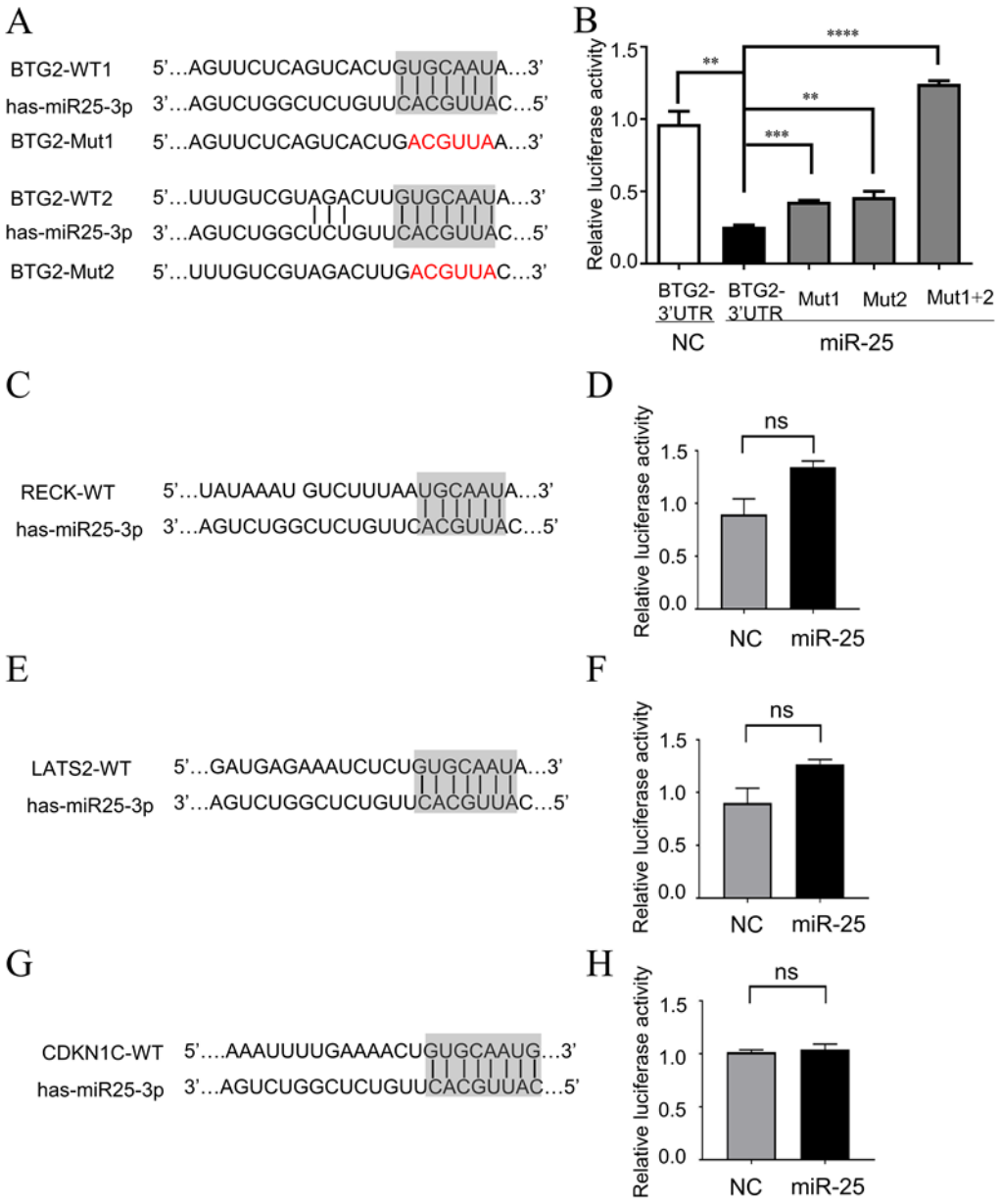

Supplemental Figure 6. The potential targets of miR-25 were tested with a dual-luciferase assay. The potential target sites (highlighted in gray) of miR-25 on the 3'-UTR of *BTG2* (A), *RECK* (C), *LATS2* (E) and *CDKN1C* (G) were predicted by TargetScan. The mutated target sequences for *BTG2* are marked in red. (B, D, F, H) Results of luciferase reporter assays for each gene (n=3, error bars show the mean ± SEM); **P<0.01; ***P<0.001; ****P<0.0001.

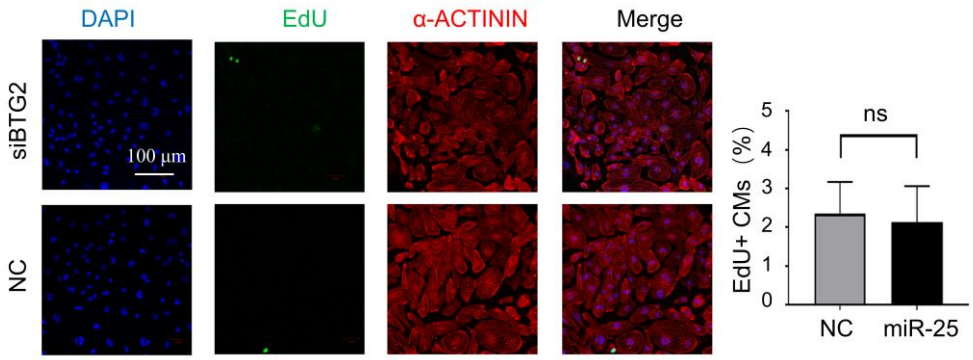

Supplemental Figure 7. Knockdown of *BTG2* had no influence on CM proliferation. EdU staining revealed that *BTG2* knockdown by siBTG2 had no influence on CM proliferation. Nuclei were stained with DAPI (blue); CMs were stained with an antibody against α-ACTININ (red). At least 2000 cells were quantified in each group.

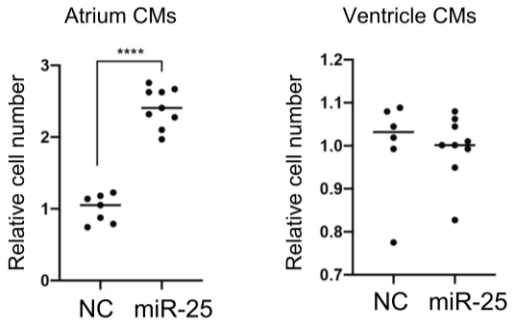

Supplemental Figure 8. miR-25 shows more significant effect on the proliferation of atrium CMs. miR-25 injection increased the atrium CMs number. A transgenic zebrafish line with myocardium-specific RFP expression in the nuclei was employed.

Table S1. Primers and oligonucleotides

Name	Sequence (5'-3')	Description
q-OCT4-F	CCTGAAGCAGAAGAGGATCACC	Primers for qPCR
q-OCT4-R	AAAGCGGCAGATGGTCGTTTGG	
q-MIXL1-F	CCCGACATCCACTTGCGCGAG	
q-MIXL1-R	GGAAGGATTTCCCACTCTGACG	
q-MESP2-F	GAACCCACCAGTGCCCTGGAC	
q-MESP2-R	TGCAGTCTCTGGCATGATGGGT	
q-NKX2-5-F	CTGTCTTCTCCAGCTCCACC	
q-NKX2-5-R	TTCTATCCACGTGCCTACAGC	
q-TNNT2-F	AAGAGGCAGACTGAGCGGGAAA	
q-TNNT2-R	AGATGCTCTGCCACAGCTCCTT	
q-FBXW7-F	GTTTGGTCAGCAGTCACAGGCA	
q-FBXW7-R	CCACACTTTGAGTGTCCGATCTG	
q-GAPDH-F	GAAGGTGAAGGTCGGAGTC	
q-GAPDH-R	GAAGATGGTGATGGGATTTC	
q-PCNA-F	CAAGTAATGTCGATAAAGAGGAGG	
q-PCNA-R	GTGTCACCGTTGAAGAGAGTGG	
q-BRCA2-F	GGCTTCAAAAAGCACTCCAGATG	
q-BRCA2-R	GGATTCTGTATCTCTTGACGTTCC	
q-NUSAP1-F	CTGACCAAGACTCCAGCCAGAA	
q-NUSAP1-R	GAGTCTGCGTTGCCTCAGTTGT	
q-RACGAP1-F	ATGCTGGCAGACTTTGTGTCCC	
q-RACGAP1-R	CAGCCAGAGATCCTATACAGGC	
q-CKS2-F	GAGGAGACTTGGTGTCCAACAG	
q-CKS2-R	GATTTGACGATCCCCAGATAAACT	
q-CCNA2-F	CTCTACACAGTCACGGGACAAAG	
q-CCNA2-R	CTGTGGTGCTTTGAGGTAGGTC	
q-CCNB-F	GACCTGTGTCAGGCTTTCTCTG	
q-CCNB-R	GGTATTTTGGTCTGACTGCTTGC	
q-CCND1-F	TCTACACCGACAACTCCATCCG	
q-CCND1-R	TCTGGCATTTTGGAGAGGAAGTG	
q-CCND2-F	GAGAAGCTGTCTCTGATCCGCA	
q-CCND2-R	CTTCCAGTTGCGATCATCGACG	
q-CDK2-F	ATGGATGCCTCTGCTCTCACTG	
q-CDK2-R	CCCGATGAGAATGGCAGAAAGC	
q-E2F2-F	CTCTCTGAGCTTCAAGCACCTG	
q-E2F2-R	CTTGACGGCAATCACTGTCTGC	
FBXW7-F	GTAATTCTAGGCGATCGCTCGAGTCAGTG GTGCAGGATGTTGG	Primers for luciferase reporter assay
FBXW7-R	TTTTATTGCGGCCAGCGGCCGCGCCCAAT GACCACTGGAGAA	
BTG2-F	GTAATTCTAGGCGATCGCTCGAGTGCTAGT	

	GCTGCTTTGTGTG	
BTG2-R	TTTTATTGCGGCCAGCGGCCGCCATCCTGG CCAAATGCCCTA	
RECK-F	GTAATTCTAGGCGATCGCTCGAG GTGCTGATGTAGCATGCTTGT	
RECK-R	TTTTATTGCGGCCAGCGGCCGC GGAAGGCCTGAAGCTCTCTC	
LATS2-F	CCGCTCGAGTACTGACAGACTGCCCACAC	
LATS2-R	GAATGCGGCCGCAGAGCGCTGTGAGTAAC AACA	
CDKN1C-F	GTAATTCTAGGCGATCGCTCGAG CGGTGAGCCAATTTAGAGCC	
CDKN1C-R	TTTTATTGCGGCCAGCGGCCGC ATAACCGAGCTAGTGCGTGG	
MT-FBXW7-F	CACGTTAAATTTCTTTATTTTCTTCTCCAG	
MT-FBXW7-R	CTGGTTTGATTTAGAAAGTCTC	
MT1-BTG2-F	ACATTGAATGCCCCCTGGGTCCCAGGA	
MT1-BTG2-R	AGTGACTGAGAACTCTTGTCC	
MT2-BTG2-F	ACATTGAATATACTGTTGTGGGTTGGA	
MT2-BTG2-R	AAGTCTACGACAAATTTGGA	
hsa-miR-25-3p mimics	5'-CAUUGCACUUGUCUCGGUCUGA-3' 5'-AGACCGAGACAAGUGCAAUGUU-3'	Oligonucleotide sequences of microRNA mimics and siRNA
mimic negative control	5'-UUCUCCGAACGUGUCACGUTT-3' 5'-ACGUGACACGUUCGGAGAATT-3'	
siFBXW7	5'-CCAAUUGUGUAGACGAUAUAC-3' 5'-GUAUAUCGUCUACACAAUUGG-3'	
siBTG2	5'-GGUCAUAGAGCUACCGUAUTT-3' 5'-AUACGGUAGCUCUAUGACCTT-3'	
siNC	5'-UUCUCCGAACGUGUCACGUTT-3' 5'-ACGUGACACGUUCGGAGAATT-3'	